ELSEVIER

Chemical Geology (Isotope Geoscience Section) 115 (1994) 283–295

CHEMICAL GEOLOGY
INCLUDING
ISOTOPE GEOSCIENCE

A comprehensive U–Pb, Sm–Nd, Rb–Sr and ^{40}Ar–^{39}Ar geochronological study on Guidong Granodiorite, southeast China: Records of multiple tectonothermal events in a single pluton

Xianhua Li

Guangzhou Branch, Institute of Geochemistry, Chinese Academy of Sciences, Guangzhou 510640, People's Republic of China

(Received February 1, 1993; revision accepted January 24, 1994)

Abstract

A complicated tectonothermal history of the Guidong Granodiorite from the Huanan Fold Belt has been revealed by using combined dating techniques. U–Pb single zircon and whole-rock Nd model ages suggest that the granodiorite was derived from an ancient crustal source which was probably composed of a mixture of 1.2–2.4-Ga crustal materials with a Nd model age of 1.6 Ga. The granodiorite emplacement age of 427 ± 3 Ma is defined by concordant U–Pb single-zircon analysis. Plagioclase, biotite, hornblende, apatite, sphene and whole rock yield an internal Sm–Nd isochron age of 428 ± 12 Ma, consistent within the analytical errors with the U–Pb zircon age. Due to the presence of inherited zircon, however, the zircon data point deviates from the Sm–Nd isochron. Four whole rocks and two mineral separates (plagioclase and hornblende) yield a Rb–Sr isochron age of 422 ± 14 Ma, which is coincident with zircon U–Pb and Sm–Nd isochron ages.

Hornblende ^{40}Ar–^{39}Ar step-heating analysis gives a main plateau age of 371.4 ± 1.3 Ma, which is considerably younger than the crystallization age. This age is interpreted as recording a post-crystallization folding event which produced the prominent unconformity between pre-Devonian and Middle Devonian strata, and resulted in the deformation of all major minerals of the granodiorite. Since most deformed minerals have remained closed to Sm–Nd and Rb–Sr isotopic migration since emplacement of the granodiorite, it can be suggested that this folding event took place without significant fluid circulation and contemporaneous metamorphism. A low-temperature heating step of hornblende yields an apparent ^{40}Ar–^{39}Ar age of 208.5 ± 2.0 Ma which may or may not have a connection to the minimum age of the Huanan Indosinian Orogeny. A biotite ^{40}Ar–^{39}Ar age spectrum yields much younger apparent ages of 145 and 92 Ma which are coincident with two important Yanshanian magmatic episodes.

1. Introduction

Isotopic study of granites is essential, not only to date their formation, but also to understand the age of source regions, cooling history of the granites, and timing of post-magmatic tectonothermal events. Different isotopic systems can record distinct age information as a result of different geochemical behaviour of parent and daughter isotopes, different closure temperatures of the isotope clocks, different retention abilities to geological disturbances and different degrees of inheritance.

Modern U–Pb single zircon dating techniques

[PD]

0009-2541/94/$07.00
SSDI 0009-2541(94)00014-Y

with low chemistry blank and sensitive high-resolution ion microprobe (SHRIMP) (e.g., Krogh, 1973, 1978; Froude et al., 1983) are best suited for granite dating. The zircon U–Pb system in granites can be complicated by the presence of inherited zircons (e.g., Pidgeon and Aftalion, 1978; Li et al., 1989; Pidgeon and Compston, 1992; Williams, 1992) and different retention of radiogenic isotopes in response to diverse geological interferences. Obviously, a complete record of granite formation and its subsequent evolution cannot be fully revealed by the U–Pb zircon system alone. Rb–Sr and K–Ar systems, which are more susceptible to post-crystallization processes, have been frequently utilized in the study of post-crystallization processes, such as cooling history of granitic plutons (e.g., Harrison and McDougall, 1980; Heizler et al., 1988), regional metamorphism (e.g., Field and Råheim, 1979), brittle deformation (e.g., Kamineni et al., 1990; Shaw and Black, 1991), ductile deformation (e.g., Black et al., 1979) and crustal uplift (e.g., Peterman et al., 1985).

The Sm–Nd system is relatively resistant to subsequent geological interferences (e.g., Faure, 1986; DePaolo, 1988), but it could be reset in some cases at high metamorphic grades (e.g., McCulloch and Black, 1984; Black, 1988; Whitehouse, 1988) or intense deformation (e.g., Gromet, 1991). Accessory and major minerals in granitic rocks usually display a large range in Sm/Nd ratios (Taylor and McLennan, 1985), which is very useful in the construction of a precise Sm–Nd isochron.

Due to the limitation by early dating techniques and the multiple regional tectonothermal activities in SE China, previously published age data for the granites from this region need to be re-examined. This paper presents a comprehensive chronological study of a granodioritic intrusion from the Huanan Fold Belt by using a variety of dating techniques including U–Pb single-zircon, whole rock–mineral Sm–Nd, whole rock–mineral Rb–Sr, and hornblende and biotite ^{40}Ar–^{39}Ar. These data are then used to discuss the genesis of this intrusion and the regional tectonothermal evolution of a part of the Huanan Fold Belt.

2. Geological setting

The southeastern part of China can be divided into three tectonic units: the Proterozoic Yangtze Craton in the north, the Huanan (=South China in Chinese) Fold Belt in the south, and the SE China Coastal Fold Belt (Ren et al., 1987). The Huanan Fold Belt has experienced repeated magmatic processes since the early Paleozoic, and granitic plutons being volumetrically dominant. Multiple intrusions of granites are characteristic from the early Paleozoic to late Mesozoic. There appears to be a rough trend of crystallization ages younging southeastwards (e.g., Jahn et al., 1976; GIG, 1979; Anonymous, 1980).

The Zhuguangshan granitoid batholith has an outcrop area of ~ 6500 km^2 within the Huanan Fold Belt along the border between the Guangdong, Hunan and Jiangxi Provinces (Fig. 1). The Guidong Granodiorite (GG) is exposed over ~ 67 km^2 on the western flank of the Zhuguangshan batholith. The GG, being intrusive to the low-grade Sinian to Cambrian metasedimentary rocks, is considered to have been emplaced during the Huanan Caledonian Orogeny, because the Zhaiqian Granite, which is transitional to the GG in terms of field relations, is unconformably overlain by Middle Devonian strata (Mo and Ye, 1980; Zhen, 1984). A poorly-defined Rb–Sr whole-rock isochron age of ~ 358 Ma for the GG has been reported by Zhen (1984).

The GG is mainly composed of 16–20% K-feldspar, 35–48% plagioclase (An_{28-42}), 20–32% quartz, 7–10% biotite and 0–4% hornblende with minor amount of magnetite, zircon, sphene, apatite and allanite. It contains many dark-coloured dioritic enclaves of 10–30 cm in length. The least altered samples have been chosen for isotopic analysis.

3. Analytical procedures

About 30 kg of sample *84-YG-79*, taken from the GG, were used for the separation of zircon and other minerals by standard mineral separation techniques — using a jaw crusher, a Frantz® isodynamic separator and heavy liquids under

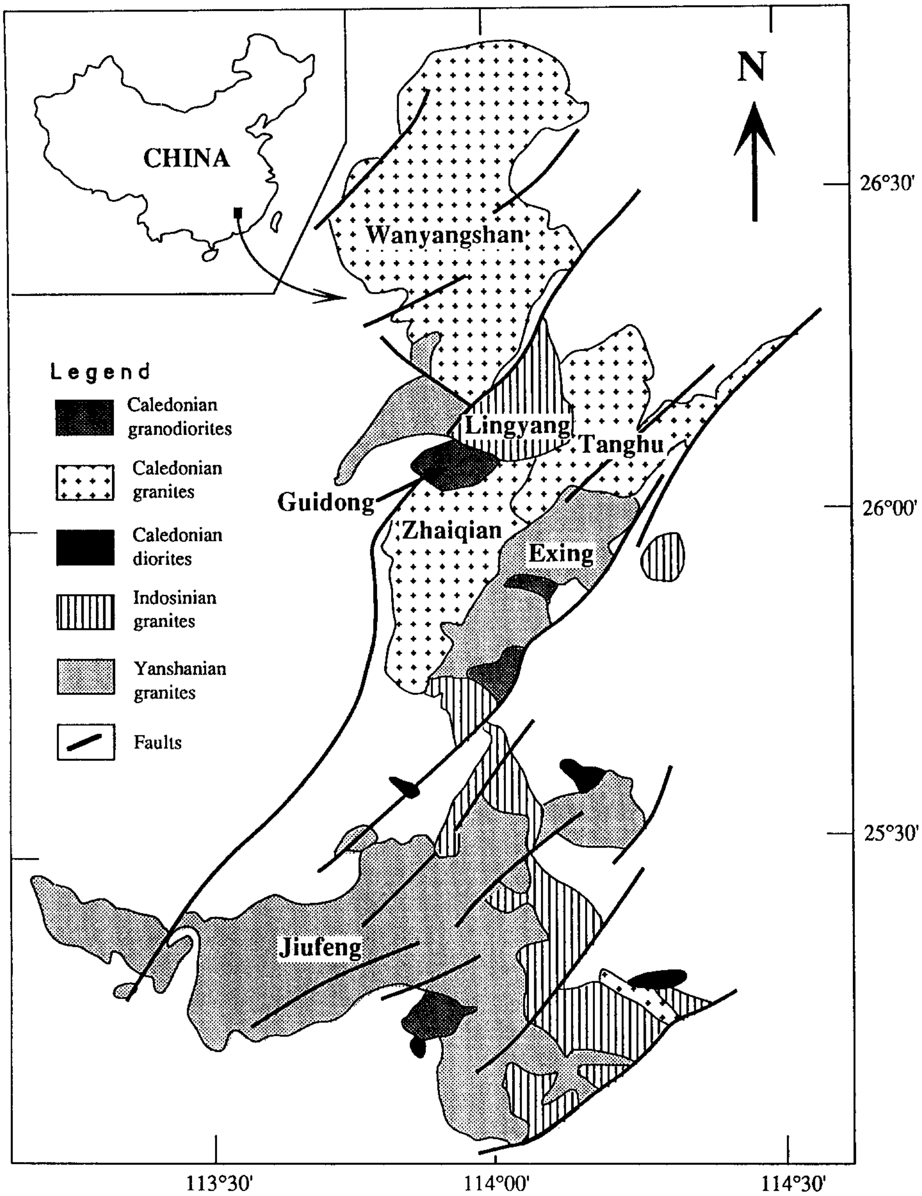

Fig. 1. Simplified geological map of the Zhuguangshan Granitic Batholith and the Guidong Granodiorite. The batholith outcrops along the border between Guangdong, Hunan and Jiangxi Provinces.

clean environmental conditions. Most zircons from the sample are light brown, euhedral to subhedral, and stubby to elongate. Some grains, however, show brown cores with light-brown or colourless turbid or thin clear overgrowths. Zircons were dissolved and U–Pb extracted using the methods of Krogh (1973, 1978). Pb and U isotopic ratios were measured on an NBS-type tandem mass spectrometer equipped with an ion pulse counter at the Denver Laboratory, Branch of Isotope Geology, U.S. Geological Survey. Total Pb blanks range from 10 to 20 pg; total U blanks are <2 pg.

Fresh rock chips were washed with distilled water in an ultrasonic bath to eliminate surface contamination. After drying, the samples were pulverized to about 200 mesh using a hardened alloy tool steel mortar and pestle. These powder samples were used for Rb–Sr and Sm–Nd analyses. Rb–Sr and Sm–Nd analytical techniques used were similar to those reported by Nakamura et al. (1976). Total blanks for a 100-mg sample are <1 ng for Sr, <0.2 ng for Rb, <0.05–0.1 ng for Nd and <0.03–0.06 ng for Sm. Neodymium, Sm and Sr were measured on an Isomass® *54*R mass spectrometer, and Rb, on an NBS-type 12-in (~30.5 cm) radius 60° mass spectrometer at the Denver Laboratory, U.S. Geological Survey. The $^{87}Sr/^{86}Sr$ and $^{143}Nd/^{144}Nd$ ratios are normalized to $^{86}Sr/^{88}Sr=0.1194$ and $^{146}Nd/^{144}Nd=0.7219$, respectively. At the time of this study, the NBS standard SRM-*987* gave a $^{87}Sr/^{86}Sr$ ratio of 0.71026 ± 0.00002 ($2\sigma_m$ uncertainties correspond to the last significant digit(s) in this study); the La Jolla standard gave a $^{143}Nd/^{144}Nd$ ratio of 0.511860 ± 0.000010.

The techniques used in the $^{40}Ar/^{39}Ar$ analyses generally followed those described by Dai et al. (1987), and the analysis was carried out at the Isotope Laboratory of the Institute of Geochemistry, Chinese Academy of Sciences. High-purity hornblende and biotite concentrates were wrapped with aluminium foil, irradiated in a swimming pool-type reactor in Chendu, along with ZBH-*25* biotite. This Chinese National Standard biotite has an ^{40}Ar–^{39}Ar age of 132.7 ± 0.1 Ma (Wang, 1983) using the decay constants and isotopic abundances recommended by Steiger and Jäger (1977). In the mass analyses, the samples were incrementally heated in an electron-bombardment furnace from 400° to 1300°C. Each heating step was maintained for 30 min. Ar isotopes were directly measured on a VG® MM-*1200* mass spectrometer after the gas was purified in a Ti furnace. Corrections for interfering Ca- and K-derived Ar isotopes, ^{36}Ar, ^{39}Ar and ^{40}Ar, were made after Dai and Hong (1982).

4. Results and discussion

4.1. U–Pb zircon system

The U–Pb zircon data of eleven zircon fractions from the GG are listed in Table 1 and shown in a concordia diagram (Fig. 2). Fractions *4–7* are two-grain analyses, and all the others are single-grain analyses. The data points are scattered and inherited radiogenic Pb isotopes in most zircon samples are clearly indicated.

The data of fractions *1–7* appear to define a discordia (*A*, Fig. 2) with lower- and upper-intercept ages of 427 ± 3 and 1224 ± 35 Ma, respectively. The lower-intercept age of 427 ± 3 Ma, which is well defined by the most concordant data point (fraction *2*, a single euhedral crystal), is interpreted as the age of granodiorite emplacement. This age also compares well with the emplacement age of 434 ± 2 Ma for the Tanghu Granite which crops out on the east flank of the Zhuguangshan batholith (Li et al., 1989). Discordia *A* probably reflects a two-component mixing system: a new magmatic zircon component (427 Ma) and an older inherited zircon component (~1.2 Ga). The upper-intercept age of 1224 Ma is consistent with the timing of the late Middle Proterozoic (1.2–1.4 Ga) crustal growth defined by U–Pb relict zircon and Nd model ages of crustal rocks in South China (Li et al., 1992). Therefore, 1224 Ma probably reflects well the age of some of the granitoid source materials.

Four other rounded zircon grains, fractions *8–11*, deviate from discordia *A*. Three reference discordia give three upper-intercept ages of ~1.4, ~1.9 and ~2.4 Ga, respectively (Fig. 2). They probably imply that some inherited zircons older than 1.2 Ga have also been involved in the source materials. Inherited zircon ages of 1.4 and 2.5 Ga have previously been obtained from the Tanghu Granite (Li et al., 1989). The age of ~1.8 Ga for relict zircons is common in the Huanan Fold Belt (Li et al., 1992). Alternatively, the deduced ages for inheritance are probably meaningless due to the large degree of discordance of these analyses which may be caused by more than one episode of Pb loss.

Table 1
U–Pb zircon isotopic data of Guidong Granodiorite, Huanan Fold Belt

Fraction[a]	Weight (mg)	U (ppm)	Pb (ppm)	$\frac{^{206}Pb_b}{^{204}Pb}$	$\frac{^{206}Pb_c}{^{238}U}$	$\frac{^{207}Pb_c}{^{235}U}$	$\frac{^{207}Pb_c}{^{206}Pb}$	Age (Ma)[d] $t_{206/238}$	$t_{207/235}$	$t_{207/206}$
1 (1, eu)	0.012	1,222	85.3	1,541	0.06886	0.5241	0.05541	427.7	429.9	428.6
2 (1, rd)	0.024	805	69.6	2,102	0.08335	0.7146	0.06218	516.1	547.5	680.3
3 (1, eu)	0.031	721	67.7	2,312	0.09365	0.8473	0.06562	577.0	623.2	794.3
4 (2, in)	0.021	657	67.9	2,490	0.08578	0.7464	0.06310	530.6	566.1	711.6
5 (2, eu)	0.020	751	54.1	951	0.06994	0.5424	0.05625	435.8	440.0	462.2
6 (2, eu)	0.015	877	62.8	941	0.06984	0.5413	0.05622	435.2	439.3	460.9
7 (2, in)	0.037	672	47.6	2,550	0.07016	0.5466	0.05650	437.1	442.8	472.2
8 (1, rd)	0.017	793	64.0	1,800	0.07981	0.6830	0.06206	495.0	528.6	676.4
9 (1, rd)	0.013	579	48.1	9,544	0.07999	0.6931	0.06284	496.1	534.6	702.9
10 (1, rd)	0.030	592	53.7	877	0.08642	0.8474	0.07112	534.3	623.2	960.9
11 (1, rd)	0.066	2,589	202.3	10,473	0.07988	0.8011	0.07273	495.4	597.4	1006.5

[a]Number in parentheses is the number of zircon grain(s) [eu = euhedral crystal; in = inclusion inside of zircon(s); rd = rounded zircon grain(s)].
[b]Measured value, corrected for mass fractionation only.
[c]Radiogenic ratios; corrected for mass fractionation, analytical Pb and U blanks, and initial common Pb. Initial Pb compositions are estimated from Stacey and Kramers (1973) at 426 Ma.
[d]Calculated ages from the corresponding radiogenic ratios, assuming $\lambda_{238} = 1.55125 \cdot 10^{-10} a^{-1}$ and $\lambda_{235} = 9.8485 \cdot 10^{-10} a^{-1}$ (Steiger and Jäger, 1977) using the ISOPLOT© program of Ludwig (1992).

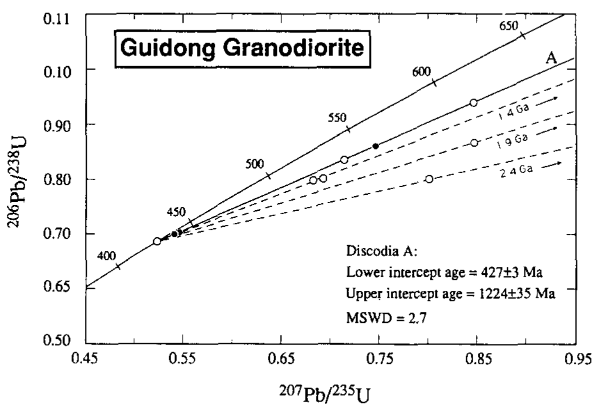

Fig. 2. Concordia diagram showing U–Pb zircon data for the Guidong Granodiorite. Scatter in the data is due to variable amounts of inherited zircon in some analyzed grains. The solid discordia *A* is defined by fractions *1–7*, and the lower- and upper-intercept ages of 427 ± 3 and 1224 ± 35 Ma, respectively. The three *dashed lines* are reference discordia linking individual inherited zircon data and the emplacement age, respectively. *Open* and *solid circles* represent single- and two-grain analyses, respectively.

4.2. Sm–Nd system

Sm–Nd isotopic ratios have been measured for whole-rock and mineral separates, including plagioclase, biotite, hornblende, apatite, sphene and zircon, from sample *84*-YG-*79*. The results are listed in Table 2 and shown in Fig. 3. $^{147}Sm/^{144}Nd$ ratios range from 0.1009 to 0.3276. Mineral separates (except zircon) and whole-rock data define an isochron (MSWD = 0.40) of 428 ± 12 Ma with an initial ϵ_{Nd}-value of −6.0 ± 0.3. This Sm–Nd isochron age is indistinguishable within analytical errors from the U–Pb zircon age of 427 ± 3 Ma, which is interpreted as the crystallization age of the granodiorite.

The zircon Sm–Nd data point clearly lies off the isochron, suggesting that not all the zircon grains are of the same generation. This is consistent with the zircon morphology and zircon U–Pb analyses described above. Unlike the other analysed minerals, the relict zircons probably preserve not only inherited U–Pb isotopic sys-

Table 2
Sm–Nd isotopic data of mineral separates and a whole rock from sample *84*-YG-*79* of Guidong Granodiorite, Huanan Fold Belt

Fraction	Sm (ppm)	Nd (ppm)	$^{147}Sm/^{144}Nd$[a]	$^{143}Nd/^{144}Nd$[a]	Age and ϵNd[b]
Whole rock	6.475	31.22	0.1252	0.512128 ± 0.000009	
Plagioclase[c]	1.140	6.831	0.1009	0.512058 ± 0.000008	
Biotite	2.596	10.57	0.1483	0.512185 ± 0.000020	428 ± 12 Ma
Hornblende	161.5	482.2	0.2017	0.512338 ± 0.000008	$\epsilon_{Nd}(T) = -6.0 \pm 0.3$
Apatite	231.7	659.2	0.2122	0.512368 ± 0.000011	(MSWD=0.40)
Sphene	293.9	715.6	0.2480	0.512475 ± 0.000012	
Zircon	7.787	14.52	0.3276	0.512572 ± 0.000013	

[a]Isotopic ratios corrected for blank and mass fractionation. The precision of $^{147}Sm/^{144}Nd$ ratios are better than $\pm 0.5\%$. Uncertainties ($2\sigma_m$) of $^{143}Nd/^{144}Nd$ ratios correspond to the last significant digit(s).
[b]Sm–Nd isochron age is calculated using the ISOPLOT© program of Ludwig (1992), excluding zircon data.
[c]Analysed at the Isotopic Laboratory, Research School of Earth Sciences, Australian National University.

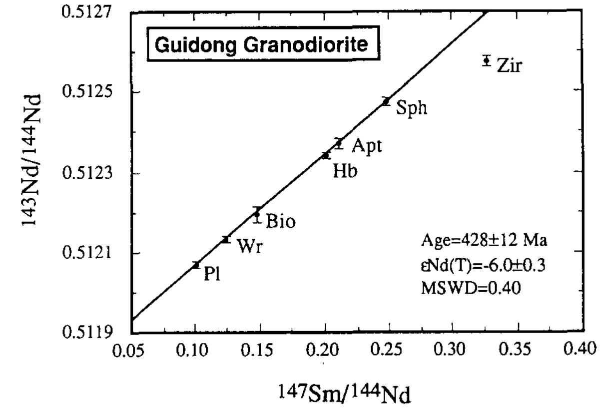

Fig. 3. Sm–Nd isochron diagram of mineral separates and whole-rock sample from Guidong Granodiorite. The isochron age (excluding zircon data) of 428 ± 12 Ma is interpreted as the emplacement age, which is indistinguishable from U–Pb zircon age within analytical errors. Sm–Nd zircon data point deviates obviously from the isochron, due to the presence of inherited zircons.

tematics, but also inherited a Sm–Nd isotopic component.

The initial ϵ_{Nd}-value of -6.0 defined by the isochron is only slightly higher than the ϵ_{Nd}(434 Ma)-values of -8.3 to -7.1 from the Tanghu Granite (Li et al., 1989). This low ϵ_{Nd}-value indicates that a significant amount of older continental crust was involved in the genesis of granodioritic magma. The whole-rock sample has a t_{DM} model age (DePaolo, 1981) of 1.6 Ga.

4.3. Rb–Sr system

Four whole-rock samples and two mineral separates (plagioclase and hornblende) have been taken for Rb–Sr isotopic analyses (Table 3; Fig. 4). Four whole-rock samples alone yield a poor-quality Rb–Sr isochron (MSWD=8.63) with an age of 423 ± 100 Ma. This large age uncertainty is mainly derived from scatter of the data points (MSWD $\gg$ 1) and small range of relative low $^{87}Rb/^{86}Sr$ ratios. Plagioclase, hornblende and whole rock from sample *84*-YG-*79* yield an internal Rb–Sr isochron (MSWD=2.19) age of 421 ± 43 Ma with an initial $^{87}Sr/^{86}Sr$ ratio of 0.7115 ± 0.0011. Data for whole-rock samples and mineral separates define an isochron (MSWD=5.5) of 422 ± 14 Ma with an initial $^{87}Sr/^{86}Sr$ ratio of 0.7115 ± 0.0004. Both internal and external Rb–Sr isochron ages are consistent within analytical errors with the zircon U–Pb and Sm–Nd isochron ages.

The present data indicate that the previous Rb–Sr whole-rock isochron age of 358 Ma (Zhen, 1984) is too young, and probably caused by the combination of a number of factors, such as analytical problems, alteration of some analysed samples and the heterogeneity of the source.

4.4. ^{40}Ar–^{39}Ar system

Hornblende and biotite concentrates were taken for ^{40}Ar–^{39}Ar analyses (Table 4; Fig. 5).

Table 3
Rb–Sr isotopic data of the Guidong Granodiorite, Huanan Fold Belt

Sample No.	Rb (ppm)	Sr (ppm)	$^{87}Rb/^{86}Sr$ [a]	$^{87}Sr/^{86}Sr$ [a]	Age and I_{Sr} [b]
G-*1*	181.9	204.7	2.309	0.72543 ± 0.00007	
82-YG-*104*	149.3	245.0	1.584	0.72105 ± 0.00006	422 ± 14 Ma
82-YG-*107*	156.9	233.8	1.944	0.72291 ± 0.00002	I_{Sr} = 0.7115 ± 0.0004
84-YG-*79*	151.0	249.0	1.757	0.72200 ± 0.00003	(MSWD = 5.5)
84-YG-*79* Pl [c]	113.4	392.9	0.836	0.71657 ± 0.00001	
84-YG-*79* Hb [c]	38.2	29.6	3.744	0.73403 ± 0.00002	

[a]The precision of $^{87}Rb/^{86}Sr$ is better than ± 1%. Uncertainties ($2\sigma_m$) of $^{87}Sr/^{86}Sr$ ratios correspond to the last significant digit.
[b]Rb–Sr isochron age is calculated using the ISOPLOT© program of Ludwig (1992).
[c]Analysed at the Isotopic Laboratory, Research School of Earth Sciences, Australian National University.

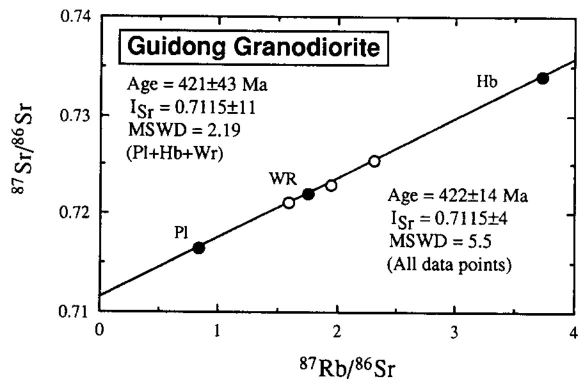

Fig. 4. Rb–Sr isochron diagram of mineral separates and whole-rock samples form the Guidong Granodiorite. Plagioclase, hornblende and whole rock from sample 84-YG-*79* (*solid symbols*) yield an internal isochron (MSWD = 2.19) with age of 421 ± 43 Ma. All of the six data (*open symbols* for other three whole-rock samples) define an isochron of 422 ± 14 Ma.

The $^{40}Ar–^{39}Ar$ apparent ages of hornblende range from 208.5 ± 2.0 to 371.4 ± 1.3 Ma. Fig. 5a shows that the age spectrum for hornblende is "disturbed" (Hanes, 1991). The main plateau, with 54.8% of total released ^{39}Ar, corresponds to an age of 371.4 ± 1.3 Ma, which is much younger than U–Pb zircon, Sm–Nd and Rb–Sr isochron ages. This $^{40}Ar–^{39}Ar$ age cannot be explained by slow-cooling history of the magma, as the granitoid plutons probably cooled quickly because they were uplifted rapidly during the Huanan Caledonian Orogeny, when most plutons were exposed at the surface, before being overlain unconformably by Middle Devonian strata with basal conglomerate layers containing the granites. Thus, the hornblende $^{40}Ar–^{39}Ar$ system, with a closure temperature of ~500°C (Harrison et al., 1979) is thought to be strongly disturbed, or reset, by a post-magmatic event.

The Silurian hiatus extended to a part of the Lower Devonian strata in much of the Huanan Fold Belt. Pre-Devonian strata and the Caledonides were overlain unconformably by Middle Devonian strata. This unconformity represents a large-scale folding event which is possibly dated by the 371-Ma $^{40}Ar–^{39}Ar$ age.

Partial radiogenic Ar loss occurred at relatively low temperatures. The first heating step with 5.83% of total released ^{39}Ar yields the youngest apparent age of 208.5 ± 2.0 Ma. The second and third steps yield apparent ages of 303.8 ± 2.1 and 331.2 ± 2.9 Ma, respectively, which are considered to be the mixing of two domains with older (371 Ma) and younger (⩽208.5 Ma?) ages. Decreasing ages over the final 28% of released argon may reflect ^{39}Ar recoil (Huneke and Smith, 1976).

Three apparent ages can be distinguished in the biotite (Fig. 5b). The low-temperature step (530°C) corresponds to the youngest age of 92 Ma with 10.4% of total ^{39}Ar. Middle-tempera-

Table 4
$^{40}Ar/^{39}Ar$ data for step-heating experiments on minerals from Guidong Granodiorite, Huanan Fold Belt

Release temperature (°C)	$\frac{^{40}Ar^*}{^{39}Ar}$	$\frac{^{40}Ar^*}{^{36}Ar}$	^{39}Ar (% of total)	^{40}Ar (%, non-atmospheric)	Apparent age (Ma)
Hornblende ($J^*=0.0012242$):					
650	100.06	686.9	5.83	50.05	208.5±2.0
765	149.82	1,614.8	7.85	82.80	303.8±2.1
870	164.56	1,658.2	2.94	82.18	331.2±2.9
970	186.67	5,184.3	54.80	95.01	371.4±1.3
1,150	172.39	5,299.0	10.60	94.48	345.5±1.6
1,280	173.30	9,053.1	16.97	96.73	347.2±1.3
1,360	176.84	2,603.3	1.01	88.64	353.6±8.3
Biotite ($J^*=0.021686$):					
520	2.42	371.1	10.41	20.31	92.3±1.4
650	3.68	1,636.8	33.48	81.76	138.4±1.9
765	3.67	1,703.4	8.25	82.47	138.0±2.0
870	3.65	3,792.2	37.39	92.55	144.8±2.1
970	3.88	1,966.3	4.70	84.79	145.8±2.3
1,070	3.84	1,824.7	2.94	83.62	144.2±2.3
1,150	3.77	996.4	1.55	70.19	141.9±3.5
1,280	3.35	530.0	1.29	47.43	126.6±3.8

ture steps (650–765°C) yield an age plateau of 138 Ma with 41.7% total ^{39}Ar. High-temperature steps (870–1150°C) give a slightly older age plateau of 145 Ma with 46.6% of total ^{39}Ar. All of the three ages are coeval with the Yanshanian (Jurassic and Cretaceous) magmatic period in Huanan.

It has been long recognized that the Yanshanian magmatic and thermal event was widespread in Huanan (e.g., Jahn, 1974; GIG, 1979; Mo and Ye, 1980; Anonymous, 1980). Our biotite ^{40}Ar–^{39}Ar date reflects the intensive Yanshanian thermal disturbance in the Caledonian granites. The pattern of the biotite ^{40}Ar–^{39}Ar age spectrum (Fig. 5b) might be explained in terms of either a slow-cooling model (Harrison and McDougall, 1982), or a multiple-event disturbance model (Harrison, 1983). In the case of slow-cooling model, the youngest apparent age of 92 Ma from the lowest-temperature step probably represents the timing of ultimate Ar closure. Alternatively, at least two ages, 145 and 92 Ma mentioned above, could be considered to temporally define discrete disturbance events. Although earlier data compiled by GCIAC (1977–1986) display a continuous age distribution for the Yanshanian granites (see also Wan and Zhu, 1991), recent high-precision data suggest that the Yanshanian magmatism in Huanan is more likely to have been mainly episodic, rather than continuous. Five main magmatic events can be recognized on the basis of reliable dating results (Jahn et al., 1976, 1986; Le Bel et al., 1984; Chen et al., 1985, 1991; Zhang et al., 1985; Zhao et al., 1985; Zhou et al., 1988, 1992; Zhu et al., 1989; Martin et al., 1991; Sewell et al., 1992; Li, 1993), i.e. Late Jurassic (155±10 Ma), Early Cretaceous (138–136 Ma and 120–125 Ma) and Late Cretaceous (100–110 and ~90 Ma). Therefore, it is probable that the biotite ^{40}Ar–^{39}Ar age spectrum records at least two thermal events during Yanshanian time at 145 and 92 Ma, corresponding to the Late Jurassic and Late Cretaceous magmatic events, respectively.

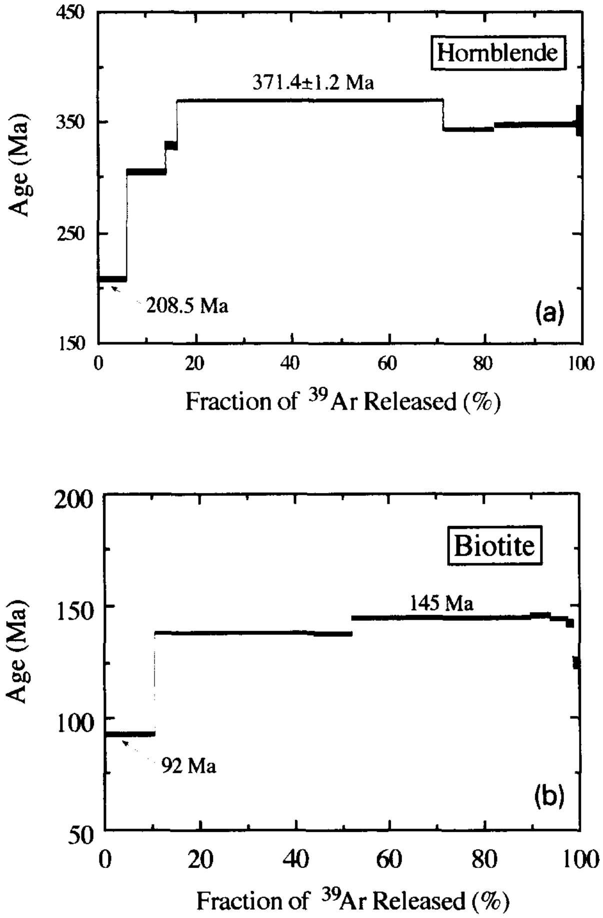

Fig. 5. ^{40}Ar–^{39}Ar apparent ages of: (a) hornblende and (b) biotite concentrations from the Guidong Granodiorite. Analytical uncertainties are represented by the bar widths.

4.5. Response of multi-chronometric systems to post-magmatic events

The refractory zircon usually has high retentivity for Pb, even at high temperatures, if there is no structural damage to the crystal lattice. Conversely, Pb can be lost from zircon through hydrothermal fluid interaction, metamorphic recrystallization, deformation, weathering and leaching. Some zircon crystals in the GG show visible micro-fractures, but such grains were not analysed in order to minimize the danger of obtaining an ambiguous age for granitic emplacement.

Agreement of Sm–Nd and Rb–Sr ages with the zircon U–Pb age demonstrates that most minerals have remained closed to post-crystallisation Sm–Nd and Rb–Sr isotopic migration, even though all the major minerals have been affected by deformation (e.g., they show wavy extinction in thin section under a polarization microscope, biotite crystals have flaky texture, and some hornblende crystals are fractured). It seems that this deformation took place without significant fluid circulation and contemporaneous metamorphism. It is rare to observe secondary mineral growth in the least altered samples.

In contrast, mineral ^{40}Ar–^{39}Ar systems in the GG exhibit distinct signs of mobility. The resetting of the hornblende ^{40}Ar–^{39}Ar clock in the GG at 371 Ma indicates that the Devonian folding event occurred either at high temperature (higher than the Ar closure temperature of $\sim 500°C$ for hornblende; Harrison et al., 1979) or at low temperature but with crystal damage, resulting in total Ar loss. The latter alternative is preferred, because the hornblende crystals experienced significant brittle deformation, and the lower Paleozoic strata were tightly folded without significant thermal metamorphism. Partial Ar loss from hornblende occurred during the Mesozoic thermal events, but the present data do not enable us to distinguish the ages of specific events. The apparent age of 208.5 Ma at the lowest heating step is somewhat ambiguous, but falls within the age range of the Triassic Huanan Indosinian Orogeny. Unlike the biotite, there is no significant Ar loss from the hornblende during the repeated Yanshanian thermal events. The difference in ^{40}Ar–^{39}Ar apparent age patterns between hornblende and biotite probably implies that the Yanshanian thermal events affected the GG with temperatures not much higher than 500°C.

Alternatively, it is probable that the Yanshanian thermal events have partially reset the K–Ar system of hornblende in the GG, and the apparent age of 208.5 Ma, and even the plateau age of 371 Ma, may have no definite geological meaning. Further work needs to define the late Paleozoic and early Mesozoic tectono-thermal events.

The biotite ^{40}Ar–^{39}Ar system has been completely reset to an early Yanshanian age, suggesting the Late Jurassic thermal event was probably the most intense during this period. Intensities of the Yanshanian thermal events in the study area seem to have decreased with time. Significant thermal events apparently ceased after 92 Ma.

5. Summary

A complicated multi-stage chronology (Fig. 6) has been registered by various isotope clocks in rocks and minerals from the Guidong Granodiorite (GG) as well as adjacent granites from Huanan.

U–Pb inherited zircon and Nd model ages suggest that the protoliths of the GG was mainly composed of a mixture of 1.2–2.4-Ga continental crustal materials with Nd model age of 1.6 Ga. In combination with available isotopic data (e.g., Li, 1993 and references therein), it could be postulated that the Huanan crustal history was initiated from the late Archean. Rapid crustal

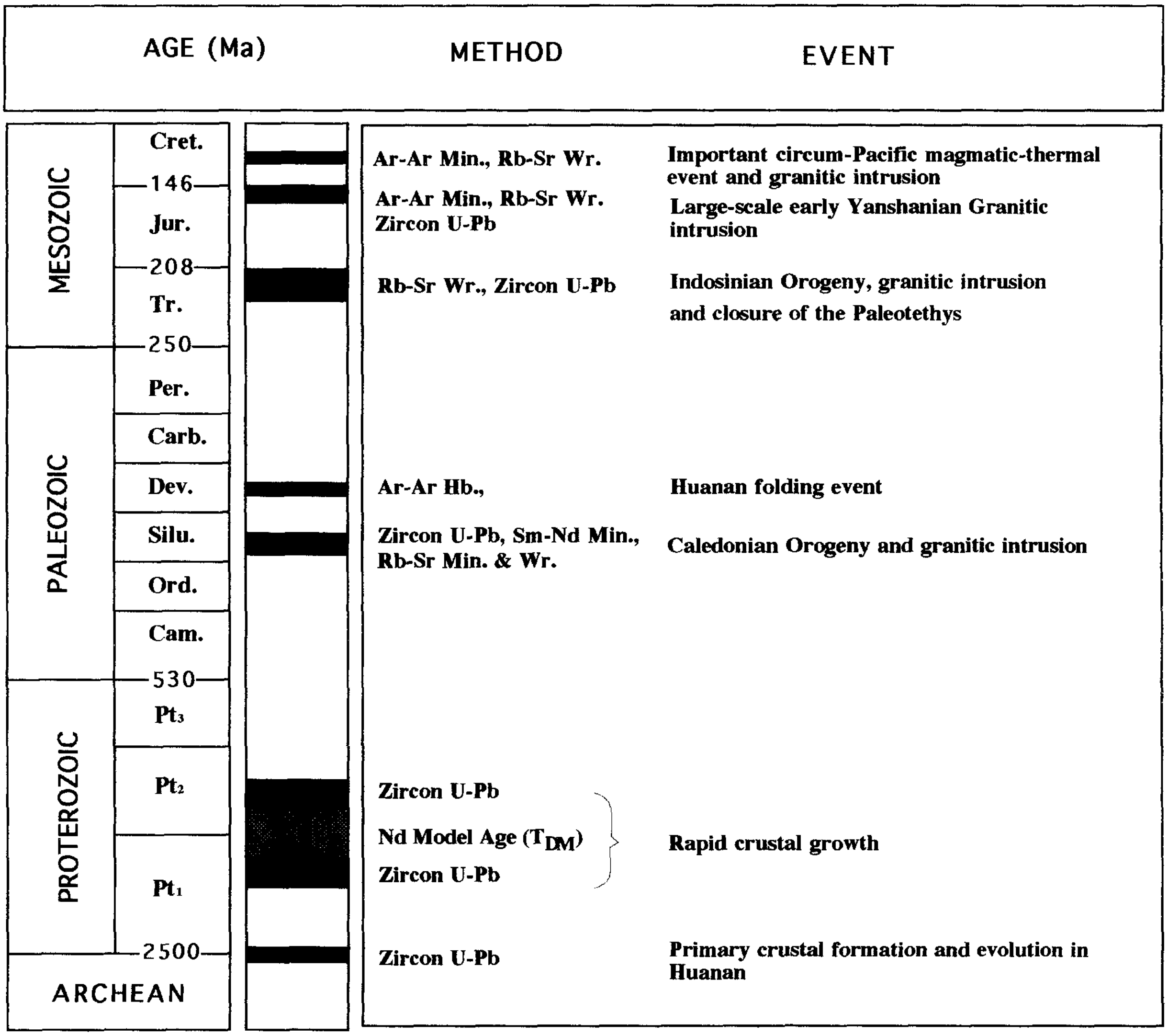

Fig. 6. Chronological history of magmatic and tectonothermal events and crustal evolution as revealed by multi-chronometric age data from the Guidong Granodiorite and adjacent granites of the Huanan Fold Belt.

growth occurred during the Middle Proterozoic, with dominant episodes at ~1.8 and 1.2–1.4 Ga.

Several recognizable magmatic- and tectonothermal episodes recorded by the GG are shown in Fig. 6. The GG was intruded during the Caledonian orogeny at ~430 Ma. Based on some poor-quality age data, the Huanan Caledonian magmatism has been traditionally divided into two subgroups (e.g., GIG, 1979; Mo and Ye, 1980), i.e. the early Caledonian (mainly Cambrian and Ordovician time) and the late Caledonian (Silurian, and extended to Middle Devonian time). In contrast, the present study and recent high-precision chronometric data (e.g., Li, 1993, and reference therein) define a restricted time span within the Silurian for the Huanan Caledonian orogeny. As there is no strong evidence for the existence of Cambrian–Ordovician granites, it appears that the age of the Huanan Caledonides should be limited mainly to the Silurian. The 370-Ma hornblende ^{40}Ar–^{39}Ar age in the GG is consistent with a distinct tectonic folding event occurring after that time.

It appears that the intensity of the Huanan Yanshanian thermal events varied temporally and spatially. There were widespread Late Jurassic granitic intrusive events in the interior of Huanan, resulting in strong thermal effects on the pre-existing granites. In contrast, Late Cretaceous granitic intrusions (~90 Ma) are mainly confined to the coastal region of the Chinese mainland and eastern Taiwan. This time is considered to be an important period of circum-Pacific magmatic–thermal events (e.g., Jahn et al., 1986).

Acknowledgements

I am greatly indebted to Tu Guangzhi, Mitsunobu Tatsumoto, Gui Xuntang and Zhu Bingquan for their advice during my Ph.D. study, and to the U.S. Geological Survey for its generous support during my research in Tatsumoto's laboratory. Dai Tongmo, W.R. Premo and O. Okano are thanked for their help with the isotopic analyses. Shen-su Sun and Jianxin Zhao are thanked for their constructive suggestions during the preparation of this paper. Malcolm McCulloch is acknowledged for giving access to the Isotope Laboratory, Research School of Earth Sciences, Australian National University, during my visit in 1992/1993. Constructive comments and critical review by B.-M. Jahn and an anonymous reviewer are gratefully appreciated.

References

Anonymous, 1980. Investigation of the time and spatial distribution of the granitic rocks of southeastern China: Their petrographic evolution, petrogenetic types and metallogenetic relations. J. Nanjing Univ. (Spec. Iss.), 56 pp.

Black, L.P., 1988. Isotopic resetting of U–Pb zircon and Rb–Sr and Sm–Nd whole-rock systems in Enderby land, Antarctica: implications for the interpretation of isotopic data from polymetamorphic and multiply deformed terranes. Precambrian Res., 38: 355–365.

Black, L.P., Bell, T.H., Rubenach, M.J. and Withnall, I.W., 1979. Geochronology of discrete structure–metamorphic events in a multiply deformed Precambrian terrain. Tectonophysics, 54: 103–137.

Chen, J., Zhou, T. and Foland, K.A., 1985. $^{40}Ar/^{39}Ar$ and Rb–Sr Geochronology of the Qingyang Batholith, Anhui Province, China. Chinese J. Geochem., 4: 220–235.

Chen, J., Zhou, T. and Yin, C. 1991. $^{40}Ar/^{39}Ar$ dating of several Mesozoic plutons in southeastern Zhejiang Province. Acta Petrol. Sin., No. 3, pp. 37–44 (in Chinese, with English abstract).

Dai, T. and Hong, A., 1982. $^{40}Ar/^{39}Ar$ dating and some isotopic determinations on Himalaya biotites from granitoid rocks in Southern Xizang. Geochimica, No. 1, pp. 48–55 (in Chinese, with English abstract).

Dai, T., Zhu, B., Zhang, Y., Pu, Z., Zhang, Q. and Hong, A., 1987. Collision and thermal history of Indian–Sundaland–Eurasian plates as implicated by $^{40}Ar/^{39}Ar$ age spectra of granodiorites. Chin. J. Geochem., 6: 33–43.

DePaolo, D.J., 1981. Nd in the Colorado Front Range and implications for crust formation and mantle evolution in the Proterozoic. Nature (London), 291: 193–196.

DePaolo, D.J., 1988. Neodymium Isotope Geochemistry — An Introduction. Springer, New York, N.Y., 187 pp.

Faure, G., 1986. Principles of Isotope Geology. Wiley, New York, N.Y., 2nd ed., 589 pp.

Field, D. and Råheim, A., 1979. Rb–Sr total rock isotope studies on Precambrian charnockitic gneiss from south Norway: evidence for isotopic resetting during a low-grade metamorphic deformational event. Earth Planet. Sci. Lett., 45: 32–44.

Froude, D.O., Ireland, T.R., Kinny, P.D., Williams, I.S., Compston, W. Williams, I.R. and Myers, J.S., 1983. Ion microprobe identification of 4100–4200 Myr-old terrestrial zircons. Nature (London), 304: 616–618.

GCIAC (Group for Collection of Isotopic Ages in China), 1977-1986. The Collection of Isotopic Ages in China, Vols. 1-4. Geological Publishing House, Beijing (in Chinese).

GIG (Guiyang Institute of Geochemistry, Academia Sinica), 1979. Geochemistry of Granitoids from South China. Science Press, Beijing, 421 pp. (in Chinese).

Gromet, L.P., 1991. Direct dating of deformational fabrics. In: L. Heaman and J.N. Ludden (Editors), Applications of Radiogenic Isotope Systems to Problems in Geology. Mineral. Assoc. Can., Short Course Handbk., 19: 167–189.

Hanes, J.A., 1991. K–Ar and $^{40}Ar/^{39}Ar$ geochronology: Methods and applications. In: L. Heaman and J.N. Ludden J.N. (Editors), Applications of Radiogenic Isotope Systems to Problems in Geology. Mineral. Assoc. Can., Short Course Handbk., 19: 27–57.

Harrison, T.M., 1983. Some observations on the interpretation of $^{40}Ar/^{39}Ar$ age spectra. Isot. Geosci., 1: 319–338.

Harrison, T.M. and McDougall, I. 1980. Investigations of an intrusive contact, northwest Nelson, New Zealand, I. Thermal, chronological and isotopic constraints. Geochim. Cosmochim. Acta, 44: 1985–2003.

Harrison, T.M. and McDougall, I., 1982. The thermal significance of potassium feldspar K–Ar ages inferred from $^{40}Ar/^{39}Ar$ age spectrum results. Geochim. Cosmochim. Acta, 46: 1811–1820.

Harrison, T.M., Armstrong, R.L., Naeser, C.W. and Harakal, J.E., 1979. Geochronology and thermal history of the Coast Plutonic complex, near Prince Rupert, British Columbia. Can. J. Earth Sci., 16: 400–410.

Heizler, M.T., Lux, D.R. and Decker, E.R., 1988. The age and cooling history of the Chain of Ponds and Big Island Pond plutons and the Spider Lake granite, west-central Maine and Quebec. Am. J. Sci., 288: 925–952.

Huneke, J.C. and Smith, S.P., 1976. The realities of recoil: ^{39}Ar recoil out of small grains and anomalous patterns in $^{40}Ar–^{39}Ar$ dating. Proc. 7th Lunar Sci. Conf., pp. 1987–2008.

Jahn, B.-M., 1974. Mesozoic thermal events in southeast China. Nature (London), 248: 480–483.

Jahn, B.-M., Chen, P.Y. and Yen, T.P., 1976. Rb–Sr ages of granitic rocks in southeastern China and their tectonic significance. Geol. Soc. Am. Bull., 87: 763–776.

Jahn, B.-M., Martineau, F., Peucat, J.J. and Cornichet, J., 1986. Geochronology of the Tananao schist complex, Taiwan, and its regional tectonic significance. Tectonophysics, 125: 103–124.

Kamineni, D.C., Stone, D. and Peterman, Z.E., 1990. Early Proterozoic deformation in the western Superior Province, Canadian Shield. Geol. Soc. Am. Bull., 102: 1623–1634.

Krogh, T.E., 1973. A low-contamination method for hydrothermal decomposition of zircon and extraction of U and Pb for isotopic age determinations. Geochim. Cosmochim. Acta, 48: 505–511.

Krogh, T.E., 1978. Vapour transfer for the dissolution of zircons in a multi-sample capsule at high-pressure. In: R.E. Zartman (Editor), Short Papers of the Fourth International Conference on Geochronology, Cosmochronology, and Isotope Geology. U.S. Geol. Surv., Open-File Rep., 78-701: 233–234.

Le Bel, L., Li, Y.D. and Sheng, J.F., 1984. Granitic evolution of the Xihuashan–Dangping tungsten-bearing system. Tschermaks Mineral. Petrogr. Mitt., 33: 149–167.

Li, X., 1993. Crustal growth and tectonic evolution in SE China: Constrains from chronological framework and isotopic systematics. Mineral. Petrol. Geochem. Lett., No. 3, pp. 111–115 (in Chinese).

Li, X., Tatsumoto, M., Premo, W.R. and Gui, X., 1989. Age and origin of the Tanghu Granite, southeast China: Results from U–Pb single zircon and Nd isotopes. Geology, 17: 395–399.

Li, X., Zhao, Z., Gui, X. and Yu, J., 1992. Sm–Nd and zircon U–Pb constraints on the age of formation of the Precambrian crust in southeast China. Chin. J. Geochem., 11: 111–120.

Ludwig, R.K., 1992. ISOPLOT — a plotting and regression program for radiogenic-isotope data, version 2.57. U.S. Geol. Surv., Open-File Rep. 91-445, 40 pp.

Martin, H., Bonin, B., Didier, J., Jahn, B.M., Lameyre, J., Qiu, Y. and Wang, Y., 1991. The Fuzhou granitic complex (SE China): Petrology and Geochemistry. Geochimica, No. 2, pp. 101–111 (in Chinese, with English abstract).

McCulloch, M.T. and Black, L.P., 1984. Sm–Nd isotopic systematics of Enderby granulites and evidence for the redistribution of Sm and Nd during metamorphism. Earth Planet Sci. Lett., 71: 46–58.

Mo, Z. and Ye, B. (Chief Compilers), 1980. Geology of Nangling Granites. Geological Publishing House, Beijing, 342 pp. (in Chinese).

Nakamura, N., Tatsumoto, M., Nunes, P.D., Unruh, D.M., Schwab, A.P. and Wildenman, T.R., 1976. 4.4 b.y.-old clast in Boulder *7*, Apollo *17*: A comprehensive chronological study by U–Pb, Rb–Sr and Sm–Nd methods. Proc. 7th Lunar Sci. Conf., pp. 2309–2333.

Peterman, Z.E., Sims, P.K., Zartman, R.E. and Schulz, K.J. 1985. Middle Proterozoic uplift events in the Dunbar dome of northeast Wisconsin, USA. Contrib. Mineral. Petrol., 91: 138–150.

Pidgeon, R.T. and Aftalion, M., 1978. Cogenetic and inherited zircon U–Pb systems in Palaeozoic granites from Scotland and England. In: D.R. Bowes and B.E. Leake (Editors), Crustal Processes and Evolution in N.W. Britain and Adjacent Regions. Geol. J., Spec. Iss., 10: 183–220.

Pidgeon, R.T. and Compston, W., 1992. A SHRIMP ion microprobe study of inherited and magmatic zircons from four Scottish Caledonian granites. Trans. R. Soc. Edinburgh, Earth Sci., 83: 473–483.

Ren, J., Jiang, C., Zhang, Z. and Qin, D., 1987. Geotectonic Evolution of China. Science Press, Beijing, 203 pp. (also published by Springer, Berlin).

Sewell, R.J., Darbyshire, D.P.F., Langford, R.L. and Strange, P.J., 1992. Geochemistry and Rb–Sr geochronology of Mesozoic granites from Hong Kong. Trans. R. Soc. Edinburgh, Earth Sci., 83: 269–280.

Shaw, R.D. and Black, L.P., 1991. The history and tectonic implications of the Redbank Thrust Zone, central Australia, based on structure, metamorphic and Rb–Sr isotopic evidence. Aust. J. Earth Sci., 38: 307–332.

Stacey, J.S. and Kramers, J.D., 1975. Approximation of terrestrial lead isotope evolution by a two-stage model. Earth Planet. Sci. Lett., 26: 207–221.

Steiger, R.H. and Jäger, E., 1977. Subcommission on Geochronology: Conventions on the use of decay constants in geo- and cosmochronology. Earth Planet Sci. Lett., 36: 359–362.

Taylor, S.R. and McLennan, S.M., 1985. The Continental Crust: Its Composition and Evolution. Blackwell, London, 312 pp.

Wan, T. and Zhu, H., 1991. Tectonic events of late Proterozoic–Triassic in South China. J. Southe. Asian Earth Sci., 6: 147–157.

Wang, S., 1983. ^{40}Ar–^{40}K and ^{40}Ar–^{39}Ar age determination on the Chinese National standard sample for K–Ar dating and its ^{40}Ar release character. Sci. Geol. Sin., No. 4, pp. 315–321 (in Chinese, with English abstract).

Whitehouse, M.J., 1988. Granulite facies Nd-isotopic homogenization in the Lewisian complex of northwest Scotland. Nature (London), 331: 705–709.

Williams, I.S., 1992. Some observations on the use of zircon U–Pb geochronology in the study of granitic rocks. Trans. R. Soc. Edinburgh, Earth Sci., 83: 447–458.

Zhang, D., Wang, X. and Sun, G., 1985. Cooling history and emplacement ages of the Guposhan–Lisong granite masses, Guangxi. Geol. Rev., 31 (3): 232–239 (in Chinese, with English abstract).

Zhao, Z., Ma, D., Lin, H. and Zhang, X., 1985. Rubidium–strontium and oxygen isotopic composition of the two types of granitoids in Yangchun area, Guangdong Province and discussion on their origin. Bull. Yichang Inst. Geol., Miner. Resour., CAGS, No. 10, 89–98 (in Chinese, with English abstract).

Zhen, J., 1984. Genesis and evolution of the Zhuguangshan granitoid batholith: Implications for the metallization. Geol. Bur. Hunan Province, Spec. Iss., 177 pp. (in Chinese).

Zhou, T., Chen, J. and Li, X., 1988. Has the Indo-Sinian magmatism occurred in Anhui Province? Acta Petrol. Sinica, No. 3, pp. 46–53 (in Chinese, with English abstract).

Zhou, T., Chen, J. and Li, X., 1992. ^{40}Ar–^{39}Ar isotopic dating of intrusions from Huoshan–Shucheng Syenite Zone, Anhui Province. Geol. Anhui, 2: 4–11 (in Chinese, with English abstract).

Zhu, J., Li, X., Shen, W., Wang, Y. and Yang, J., 1989. Sr, Nd and O isotopic study on the genesis of the Huashan granitic complex, Guangxi. Acta Geol. Sin., 63(3): 225–235 (in Chinese, with English abstract).